Diffuse reflectance spectroscopy for *in vivo* pediatric brain tumor detection

Wei-Chiang Lin
Miami Children's Hospital
    and
Florida International University
Department of Biomedical Engineering
10555 West Flagler Street, EAS 2673
Miami, Florida 33131

David I. Sandberg
Sanjiv Bhatia
Miami Children's Hospital
    and
University of Miami Leonard M. Miller School of
    Medicine
Department of Neurological Surgery
3215 SW 62nd Avenue
Ambulatory Care Building, Suite 3109
Miami, Florida 33155

Mahlon Johnson
University of Rochester Medical Center
Department of Pathology
Division of Neuropathology, Box 626
601 Elmwood Avenue
Rochester, New York 14642

Sanghoon Oh
Miami Children's Hospital
    and
Florida International University
Department of Biomedical Engineering
10555 West Flagler Street, EAS 2673
Miami, Florida 33131

John Ragheb
Miami Children's Hospital
    and
University of Miami Leonard M. Miller School of
    Medicine
Department of Neurological Surgery
3215 SW 62nd Avenue
Ambulatory Care Building, Suite 3109
Miami, Florida 33155

Abstract. The concept of using diffuse reflectance spectroscopy to distinguish intraoperatively between pediatric brain tumors and normal brain parenchyma at the edge of resection cavities is evaluated using an *in vivo* human study. Diffuse reflectance spectra are acquired from normal and tumorous brain areas of 12 pediatric patients during their tumor resection procedures, using a spectroscopic system with a hand-held optical probe. A total of 400 spectra are acquired at the rate of 33 Hz from a single investigated site, from which the mean spectrum and the standard deviation are calculated. The mean diffuse reflectance spectra collected are divided into the normal and the tumorous categories in accordance with their corresponding results of histological analysis. Statistical methods are used to identify those spectral features that effectively separated the two tissue categories, and to quantify the spectral variations induced by the motion of the handheld probe during a single spectral acquisition procedure. The results show that diffuse reflectance spectral intensities between 600 and 800 nm are effective in terms of differentiating normal cortex from brain tumors. Furthermore, probe movements induce large variations in spectral intensities (i.e., larger standard deviation) between 400 and 600 nm. © *2010 Society of Photo-Optical Instrumentation Engineers.* [DOI: 10.1117/1.3505012]

1 Introduction

Brain tumors are the second most common malignancy and the leading cause of death from cancer in children. Yearly, more than 2000 children are diagnosed with a brain tumor in the United States, and 30,000 to 40,000 are diagnosed worldwide.[1,2] The three most common pediatric brain tumors are astrocytoma ($\sim$ 42%), medulloblastoma (16.3%), and ependymoma (10.1%).[3] Although dysembryoplastic neuroepithelial tumors are benign, congenital tumors, they occur frequently in children and have a high association with seizures. For each of these pathological entities, gross total surgical resection, when feasible, is the optimal initial treatment option.[4] A strong correlation between the extent of tumor resection and clinical outcomes, such as 10-yr, progression-free survival, has been reported by different groups.[5–9]

To achieve a maximal tumor resection, an accurate delineation of the margins of the brain tumor during the planning and surgical stages is required. Similar to the adult population, preoperative tumor diagnosis and volumetric analysis for the pediatric brain tumor population are achieved using advanced

Address all correspondence to: Wei-Chiang Lin, Florida International University, Department of Biomedical Engineering, 10555 West Flagler St., EAS 2673, Miami, FL 33131. Tel:305-348-6112; Fax: 305-348-6954; E-mail: wclin@fiu.edu.

imaging modalities, especially magnetic resonance imaging[10] (MRI). For certain tumor types, their physiological characteristics are assessed further by the use of magnetic resonance spectroscopy and positron emission tomography.[11–13] Frameless stereotaxy is used commonly to relay this preoperative diagnostic information into a surgical field.[14,15] In addition to the fact that preoperative imaging studies are limited in their ability to define the true pathological margins of the brain tumor,[16] the surgical navigation systems may become inaccurate during surgical procedures due to shifting of brain structures.[17–19] Ultrasonography is another popular intraoperative means for guiding tumor resection.[16,20–22] Ultrasound, however, is less likely to differentiate tumor from peritumoral edema, which is also hyperechoic.[20,21] Intraoperative MRI can also be used to assess tumor resection intraoperatively. However, obtaining multiple MRI scans during tumor resections is impractical. Therefore, newer technologies are being developed continuously to make surgery safer and more efficient.

The concept of using the tissue differentiation ability of optical spectroscopy to guide brain tumor surgery has been explored over the past 15 yr. So far, several researchers have successfully demonstrated the feasibility of using optical spectroscopy to differentiate brain tumors from normal brain tissue *in vitro* and *in vivo*.[23–32] While the results are promising, all of these studies with one exception were conducted only on adult brain tumor patients. The *in vivo* applicability of such a technique for pediatric brain tumor patients has not been evaluated previously. Similar to the majority of *in vivo* tissue diagnostic studies, optical spectral acquisition from the *in vivo* brain often is achieved using a handheld optical probe. The potential spectral alterations induced by the movements of a handheld probe have not been investigated thoroughly. Here, a small-scale, clinical study was conducted on the children with brain tumors to evaluate the feasibility of using diffuse reflectance spectroscopy to differentiate brain tumors from normal brain tissue. Concurrently, the quality of *in vivo* diffuse reflectance spectra acquired using a handheld probe was evaluated via repeated spectral acquisition from a single investigated site.

2 Materials and Methods

2.1 *Instrumentation*

A fiber optic spectroscopic system was used to acquire diffuse reflectance spectra from the brains of pediatric brain tumor patients who were undergoing craniotomies for tumor resection. The system was similar to those reported in previous studies.[24,30] It consisted of a light source, a fiber optic probe, a spectrophotometer, and a computer station with control software. The light source was a tungsten halogen light (LS-1, Ocean Optics, Dunedin, Florida) with a spectral bandwidth of 360 to 2000 nm and an output power of 6.5 W. The fiber optic probe was custom designed and manufactured by RoMack Fiber Optics, Inc. (Williamsburg, Virginia), and it contained seven 300-μm-core-diam fibers with a 0.22 numerical aperture. One of the seven fibers was allocated for excitation light conduction, and five were allocated for backscattered light collection and conduction. The seventh fiber was designed for a second excitation light source (e. g., laser), which was not used here. The spectrometer (USB2000, Ocean Optics, Dunedin, Florida) of the system had

a 2048-element linear CCD array detector with a 12-bit resolution, and its spectral range was from 240 to 932 nm. The data acquired by the spectrometer were transferred to the computer station through a universal serial bus. The computer station (Inspiron E1405, Dell, Austin, Texas) with control software was used to operate the spectrophotometer and to store the acquired spectral data. The control software, programmed using Lab VIEW 8.2 (National Instruments, Austin, Texas), automated the spectral acquisition process, and the software initiated a spectral acquisition by sending a trigger signal to the spectrometer.

2.2 *Clinical Study*

A small-scale clinical study was conducted at Miami Children's Hospital to evaluate the feasibility of using diffuse reflectance spectroscopy to differentiate pediatric brain tumors from normal brain tissue in an intraoperative setup. The protocol for this clinical study was reviewed and approved by the Western Institutional Review Board and the Institutional Review Board of Florida International University. Informed consent and assent were obtained from each participant and her or his parents. Assent was obtained from the participants between 7 and 18 years of age. The recruitment of study subjects was conducted by the three neurosurgeons involved in this study (JR, SB, and DS).

During an *in vivo* spectral acquisition procedure, the optical probe, held by the neurosurgeon, was placed in direct contact with the brain area to be investigated. The probe contact pressure was maintained at a level for which brain deformation was not visible. The investigated sites were selected from normal brain area (i.e., far away from the resection zone) and from tumor tissue. From each investigated site, a set of 400 diffuse reflectance spectra was acquired at the rate of 33 Hz (i.e., integration time = 30 ms). The baseline spectrum was acquired sequentially to gauge the interference of the room light. Biopsy samples were taken only from the investigated sites within the resection zone for further histological evaluation. Note biopsy samples were not take from the normal brain area because of the ethical reasons.

2.3 *Histology*

Histological evaluations were conducted for all biopsy samples obtained from this study. These biopsy samples were fixed in formalin and then subjected to routine sectioning and staining. Three 5-μm sections were cut from each specimen, and they were stained with hematoxylin and eosin (H&E). The prepared tissue sections were reviewed by a neuropathologist (MJ), who was blinded to all clinical information. Abnormal microscopic features of each sample were documented, and these features were then used to categorize the spectral data set in the spectral data analysis procedure.

2.4 *Data Processing and Analysis*

Prior to data analysis, the collected diffuse reflectance spectra were preprocessed to remove spectral artifacts and reduce the size of the spectral data. Specifically, the baseline subtraction and the application of the calibration factors, as described in previous publications,[24,30] were conducted sequentially for each diffuse reflectance spectrum. The spectral range of the processed spectra was reduced to 400 to 850 nm with 5-nm increments.

For each site that was investigated, the mean spectrum $Rd_{m,\text{site}}(\lambda)$ and the standard deviation $\text{STD}_{\text{site}}(\lambda)$ were calculated from its corresponding spectral data set. To reduce the effect of biological variations among the patients studied, a spectral normalization method was employed. Specifically, $Rd_{m,\text{site}}(\lambda)$ from a single patient were normalized to the average maximum intensity of the normal measurements from the same patient, which yielded $nRd_{m,\text{site}}(\lambda)$. Then, $nRd_{m,\text{site}}(\lambda)$ from all investigated sites were further divided into two categories, a normal group and a tumorous group, in accordance with their corresponding histopathological identities. To identify the representative spectral features, the average spectral intensities of the two groups were compared at all wavelengths using Student's t test with a significance level of $\alpha = 0.05$. The classification effectiveness of the representative spectral features was further evaluated using the area under the receiver operating characteristic (ROC) curve method in the statistical software package SPSS (SPSS Inc, Chicago, Illinois). Empirical discrimination algorithms were developed using the spectral features with the area under the ROC curve A_{ROC} that is greater than 0.7.

Analyses were also conducted on $\text{STD}_{\text{site}}(\lambda)$ to quantify the spectral intensity variations induced by the handheld probe. To facilitate this process, a new index $\%\text{STD}_{\text{site}}(\lambda)$ was created, and it is calculated based on

$$\%\text{STD}_{\text{site}}(\lambda) = [\text{STD}_{\text{site}}(\lambda) \, / \, Rd_{m,\text{site}}(\lambda)] \times 100 \, (\%).$$

The $\%\text{STD}_{\text{site}}(\lambda)$ values from all investigated sites also were classified into two groups, i.e., normal and tumorous groups, and the statistically significant differences between the mean $\%\text{STD}_{\text{site}}(\lambda)$ of the two groups at all wavelengths were compared using the Student's t test. The wavelength dependence of $\%\text{STD}_{\text{site}}(\lambda)$ was also analyzed for each tissue category.

3 Results

A total of 12 patients was enrolled in the clinical trial reported here (Table 1). All studies were conducted successfully, and there were no unexpected complications. Nine of the 12 patients were females, and three were males. Eight patients had tumors in the cerebrum, and four had tumors in the cerebellum. The tumor types studied encompassed the major pediatric brain tumor categories, including pilocytic astrocytoma, ganglioglioma, and medulloblastoma (Table 2). Overall, 32 measurements were performed on the normal sites (i.e., cerebral cortex and cerebellar cortex) and 27 measurements were performed on the tumor sites. Since only a few measurements were obtained from white

Table 1 Demographic information of studied patients.

| Age	Count	Gender	Count
<1	2	Male	3
1–5	1	Female	9
6–10	6		
11–15	3		

Table 2 Distribution of studied tumor types and investigated sites.

| Brain Tissue Category	Number of Measurements	Tumor Category	Number of Patients
Cerebral cortex	20	Pilocytic astrocytoma	5
Cerebellar cortex	12	Ganglioglioma	2
Tumor	27	Chondrosarcoma	1
		Medulloblastoma	2
		High-grade malignancy	1
		Monomorphous angiocentric glioma	1

matter, these measurements were excluded from the statistical analysis.

The representative diffuse reflectance spectra from normal and tumorous brain tissues are shown in Fig. 1. The most noticeable difference observed between these spectra is that the intensities from normal brain tissues were greater than the intensities of tumor tissues. It was found that diffuse reflectance spectra from pediatric brain tissues had profile features that were similar to those from adult brain tissues. The dominant feature in these diffuse reflectance spectra is the absorption characteristics of hemoglobin; the absorption peaks of hemoglobin in the visible wavelength region yield the two valleys in the wavelength region between 400 and 600 nm.

The Student's t test (two-sided, equal variance) was used to detect any significant differences between the average intensities of $nRd_{m,\text{site}}(\lambda)$ obtained from normal brain tissue and that obtained from tumor tissues at a given wavelength. The results of the statistical comparisons, presented by p values, are shown in Fig. 2. Statistically significant differences ($p < 0.05$) were observed in three spectral regions: 450 to 530, 590 to 690, and beyond 800 nm. Because of the high noise level, the differences beyond 800 nm were considered to be of questionable significance. The same statistical comparison was performed
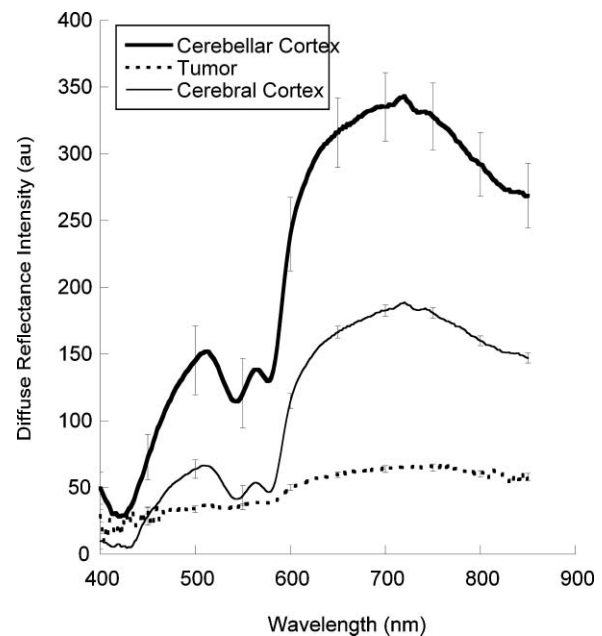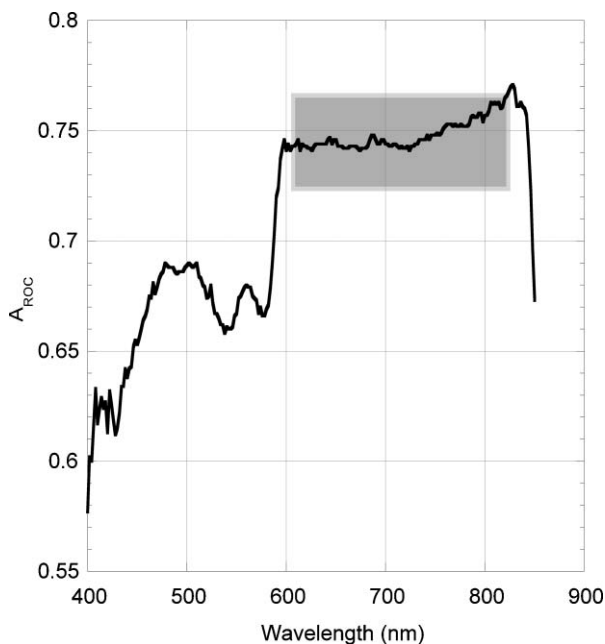

Fig. 1 Representative $Rd_{m,\text{site}}(\lambda)$ from cerebral cortex (thick solid line), cerebella cortex (thin solid line), and brain tumor (dotted line). The error bars represent the $\text{STD}_{\text{site}}(\lambda)$.
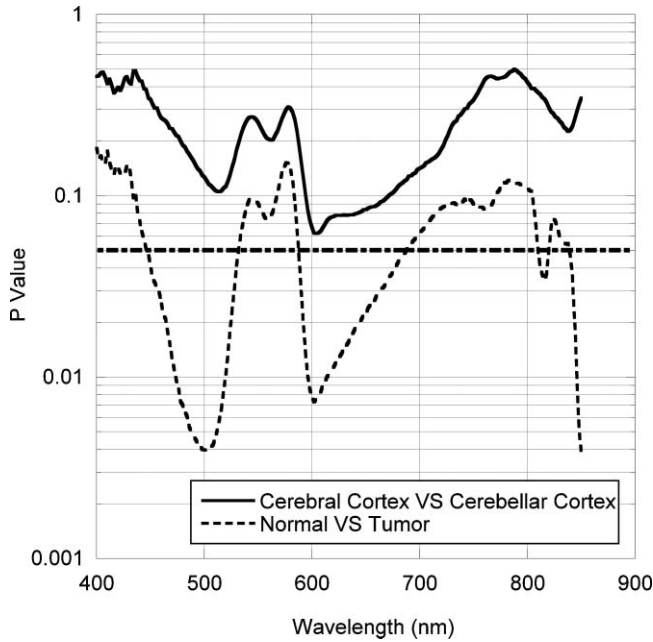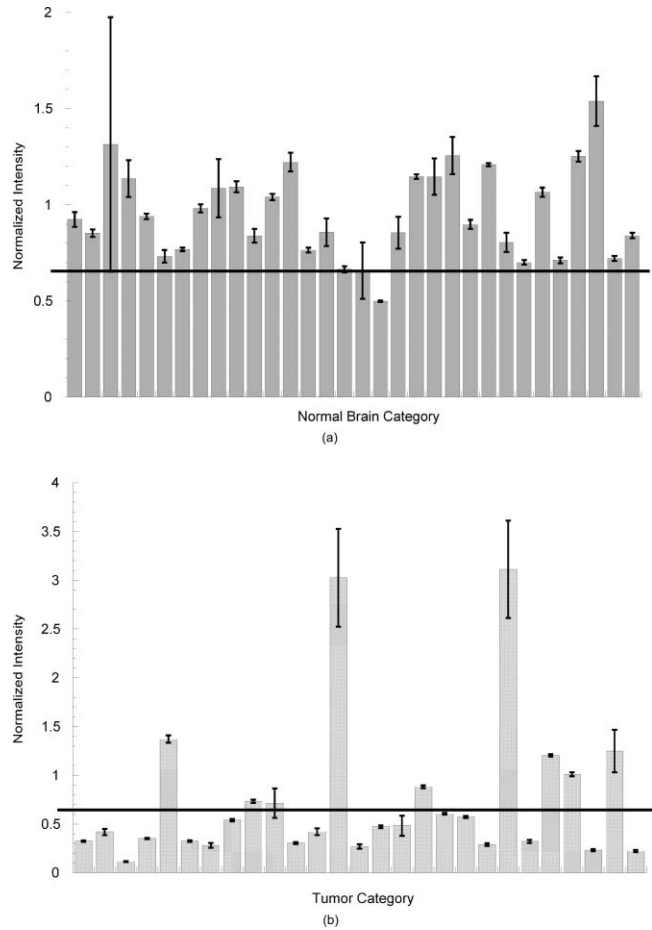
Fig. 2 Results of the Student's *t* test of the average diffuse reflectance intensities between (a) the normal and the tumorous groups (dashed line) and (b) cerebral and cerebellar cortex (solid line). The horizontal line indicates the significance level $\alpha = 0.05$.

between the average intensities of $nRd_{m,\text{site}}(\lambda)$ from the cerebral and cerebellar cortex. However, no significant differences were detected (Fig. 2).

The outcome of the area under the ROC curve analysis is summarized in Fig. 3. It was noted that, in general, greater A_{ROC} values were found in the longer wavelength region (i.e., 600 nm to 830 nm). The maximum A_{ROC} obtained was 0.77, which was located at $\sim$820 nm.


Fig. 4 Results for $nRd_{m,\text{site}}(700 \text{ nm})$ from (a) normal brain samples and (b) brain tumor samples. The error bars represent $\text{STD}_{\text{site}}(700 \text{ nm})$. The black line is an arbitrary cutoff (0.65) established for the purpose of discrimination; brain samples with $nRd_{m,\text{site}}(700 \text{ nm})$ greater than the cutoff are classified as normal.

Fig. 3 Graph of $A_{\text{ROC}}(\lambda)$ from the area under the ROC curve analysis.

To demonstrate the effectiveness of the identified spectral features (i.e., normalized diffuse reflectance intensity) for differentiating brain tumor tissue from normal brain tissue, one representative spectral feature, $nRd_{m,\text{site}}$ (700 nm), was used to construct an empirical discrimination method. This discrimination method produced a sensitivity of 95% and a specificity of 66%, using an arbitrary cutoff of 0.65 (Fig. 4). A similar performance was obtained from the discrimination algorithms, using a single $nRd_{m,\text{site}}(\lambda)$ between 600 and 830 nm as the input.

The analysis of $\%\text{STD}_{\text{site}}(\lambda)$ provides insights into the spectral variations induced by the handheld probe. As shown in Fig. 5, the average $\%\text{STD}_{\text{site}}(\lambda)$ varied from 10 to 50% between 400 nm and 850 nm, and the maximum $\%\text{STD}_{\text{cat}}(\lambda)$ was observed close to 400 nm. It was also noticed that the values of $\%\text{STD}_{\text{site}}(\lambda)$ below 600 nm were, in general, much greater than the values above 600 nm. Interestingly, the profile of the average $\%\text{STD}_{\text{site}}(\lambda)$ of each tissue category strongly resembles the absorption spectrum of oxyhemoglobin. According to the Student's *t* test, the difference in the average $\%\text{STD}_{\text{site}}(\lambda)$ between the normal brain category and the brain tumor category was not statistically significant.
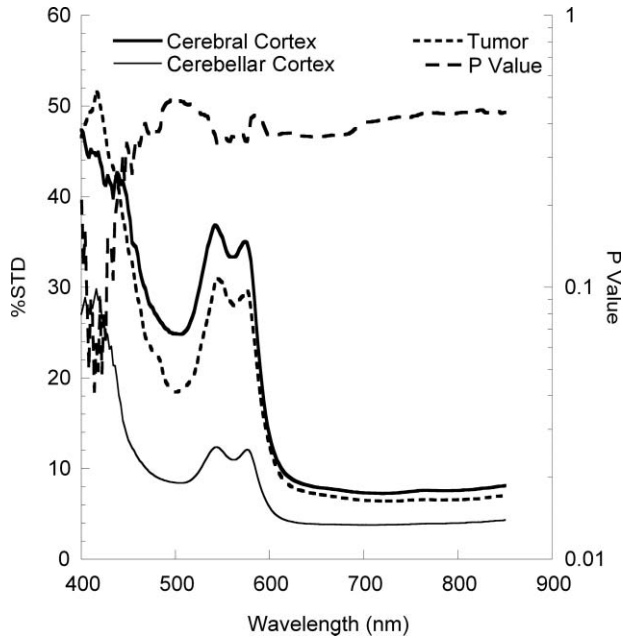
Fig. 5 Average $\%STD_{site}(\lambda)$ of cerebral cortex (thick solid line), cerebellar cortex (thin solid line), and brain tumor (dotted line). The upper dashed line represents the *t* test results between the normal brain (i.e., cerebral + cerebellar cortex) and brain tumor groups.

4 Discussion

The results from the clinical study reported in this paper suggest that pediatric brain tumors may be differentiated from the normal brain *in vivo* using diffuse reflectance spectroscopy alone. Statistical comparisons identify several wavelength regions where diffuse reflectance intensities from normal brain differ from those of brain tumors. Without employing sophisticated spectral analysis and classification tools, we were able to construct an empirical discrimination method, based on one single spectral feature, with reasonably high accuracy. Despite the small number of patients enrolled in this study, we believe the results strongly support the feasibility of using diffuse reflectance spectroscopy to identify brain tumors *in vivo* and, hence, guide a pediatric brain tumor surgery.

In vivo diffuse reflectance signals from cerebral cortex were found to be higher than those from brain tumors over the spectral region recorded. This observation is inconsistent with the findings of the adult brain tumor studies.[31,33] Both Gebhert et al. and Eggert and Blazek reported that the scattering properties of adult brain tumors were stronger than those from cerebral cortex. Therefore, it is expected that the diffuse reflectance signals between 600 and 800 nm from adult brain tumor should be stronger than those from cerebral cortex. The discrepancy, in our opinion, should be attributed to the structural/composition differences between adult and pediatric brain tumors. Therefore, optical surgical guidance developed for adult brain tumors would not be directly applicable to the pediatric brain tumor population.

In this study, diffuse reflectance signals were also measured from the cerebellar cortex, and they were comparable with those from cerebral cortex in terms of spectral intensity and profile. Therefore, a separate classification algorithm for cerebellar cortex, cerebellar tumors did not have to be created. Because the number of measurements from white matter was relatively low, they were not included in the statistical comparisons disclosed in the result section. Nevertheless, we are certain about the feasibility of using the same spectral features, namely, $nRd_{m,site}(\lambda)$ for $\lambda = [600 \text{ nm}, 800 \text{ nm}]$, to differentiate cerebral and cerebellar white matter from pediatric brain tumors with high efficiency. This assessment is supported by several previously published studies that showed that diffuse reflectance signals from white matter are notably stronger than those from the cerebral cortex due to its high scattering characteristic. The strong scattering properties of white matter have been attributed to the dimension and density of neural axons as well as neural myelination.[33]

The two spectral regions showing statistically significant differences between normal cortex and tumor tissue are 450 to 530 and 590 to 690 nm. However, the analysis of A_{ROC} suggests that diffuse reflectance signals beyond 600 nm are more suitable discriminants. This discrepancy can be explained by the distribution characteristics of $nRd_{m,site}(\lambda)$ from the tumorous group. As shown in Fig. 4(b), the $nRd_{m,site}(\lambda)$ of two samples significantly deviate from the group mean. In other words, these two samples would introduce a strong bias to the distribution of $nRd_{m,site}(\lambda)$ of the tumorous group, thus degrading the results of mean comparison (i.e., increasing the *p* value). According to the histological evaluation, both samples belong to the ganglioglioma tumor category, which suggests a separate tissue discrimination algorithm may be developed for this particular tumor type. Note also that diffuse reflectance spectral signal from ganglioglioma is stronger than those from the other specimens over the entire spectral region. Future studies with a larger number of patients in each histological category will be required to ensure this conclusion.

One issue associated with the utility of the handheld probe is its stability. The investigated site as well as the probe contact pressure vary because of the movements of the investigated organ (e. g., brain pulsation) and/or the operator's hand. This instability may affect *in vivo* diffuse reflectance spectral acquisition in two distinct ways. First, the lateral movement of the handheld probe causes a shift in the investigation location; thus, the resulting spectrum represents the characteristics of a tissue volume greater than expected. This in turn introduces more errors to the process of correlating the histologic findings with the spectral data. Second, the axial movement of the probe induces irregularity in the probe contact pressure, which primarily leads to a significant change in tissue hemodynamics. As reported by several research groups, [34,35] excessive probe contact pressure can lead to significant changes in local tissue hemodynamics, which explains the high %STD in the region of hemoglobin absorption, as shown in Fig. 5. Therefore, the spectral features below 600 nm are not reliable inputs for the tissue discrimination purpose. In a separately study which is not yet published, we noticed that the usage of a handheld probe in conjunction with a mechanical holder can significantly reduce %STD. Such an improvement enables continuous recording of diffuse reflectance spectra from the brain, which is important for applications such as studying the temporal dynamics of epileptic cortex.

5 Conclusion

We investigated the utility of diffuse reflectance spectroscopy for *in vivo* pediatric brain tumor detection using a small-scale

clinical trial. The results of the study found that pediatric brain tumors may be differentiated from normal cortex using spectral features such as diffuse reflectance intensity between 600 and 800 nm. Because of the high scattering properties of the white matter, the same differentiation efficient should be expected between white matter and pediatric brain tumors. Spectral artifacts induced by the handheld probe also were quantified by studying the standard deviations of diffuse reflectance spectra continuously acquired at the same investigated site. It was found that large intensity variations exist in the spectral region of 400 to 650 nm in the repeatedly measured diffuse reflectance spectra. This in turn diminishes the applicability of the spectral features from this wavelength region to the discrimination algorithm development.

Acknowledgments

References

1. R. T. Baldwin and S. Preston-Martin, "Epidemiology of brain tumors in childhood—a review," *Toxicol. Appl. Pharmacol.* **199**(2), 118–131 (2004).
2. "Cancer Facts & Figures 2005," American Cancer Society (2005).
3. N. J. Ullrich and S. L. Pomeroy, "Pediatric brain tumors," *Neurol. Clin.* **21**(4), 897–913 (2003).
4. J. T. Rutka and J. S. Kuo, "Pediatric surgical neuro-oncology: current best care practices and strategies," *J. Neurooncol.* **69**(1–3), 139–150 (2004).
5. C. Fernandez, D. Figarella-Branger, N. Girard, C. Bouvier-Labit, J. Gouvernet, A. Paz Paredes, and G. Lena, "Pilocytic astrocytomas in children: prognostic factors—a retrospective study of 80 cases," *Neurosurgery* **53**(3), 544–553; discussion 554–555 (2003).
6. I. F. Pollack, D. Claassen, Q. al-Shboul, J. E. Janosky, and M. Deutsch, "Low-grade gliomas of the cerebral hemispheres in children: an analysis of 71 cases," *J. Neurosurg.* **82**(4), 536–547 (1995).
7. J. F. Hirsch, C. Sainte Rose, A. Pierre-Kahn, A. Pfister, and E. Hoppe-Hirsch, "Benign astrocytic and oligodendrocytic tumors of the cerebral hemispheres in children," *J. Neurosurg.* **70**(4), 568–572 (1989).
8. E. R. Laws, Jr., W. F. Taylor, M. B. Clifton, and H. Okazaki, "Neurosurgical management of low-grade astrocytoma of the cerebral hemispheres," *J. Neurosurg.* **61**(4), 665–673 (1984).
9. S. Mercuri, A. Russo, and L. Palma, "Hemispheric supratentorial astrocytomas in children. Long-term results in 29 cases," *J. Neurosurg.* **55**(2), 170–173 (1981).
10. L. G. Vezina, "Imaging of central nervous system tumors in children: advances and limitations," *J. Child Neurol.* **23**(10), 1128–1135 (2008).
11. A. Panigrahy, M. D. Krieger, I. Gonzalez-Gomez, X. Liu, J. G. McComb, J. L. Finlay, M. D. Nelson, Jr., F. H. Gilles, and S. Bluml, "Quantitative short echo time 1 H-MR spectroscopy of untreated pediatric brain tumors: preoperative diagnosis and characterization," *AJNR Am J. Neuroradiol.* **27**(3), 560–572 (2006).
12. S. Patil, L. Biassoni, and L. Borgwardt, "Nuclear medicine in pediatric neurology and neurosurgery: epilepsy and brain tumors," *Semin. Nucl. Med.* **37**(5), 357–381 (2007).
13. H. Jadvar, L. P. Connolly, F. H. Fahey, and B. L. Shulkin, "PET and PET/CT in pediatric oncology," *Semin. Nucl. Med.* **37**(5), 316–331 (2007).
14. R. J. Maciunas, *Approaches to Frame-Based and Frameless Stereotaxis*, Thieme Medical, New York (1997).
15. R. J. Maciunas, "Pitfalls," in *Image-Guided Neurosurgery: Clinical Applications of Surgical Navigation*, G. H. Barnett, D. W. Roberts, and R. J. Maciunas, Eds., pp. 43–60, Quality Medical, St. Louis, MO (1998).
16. P. LeRoux, T. Winter, M. Berger, L. Mack, K. Wang, and J. Elliott, "A comparison between preoperative magnetic resonance and intraoperative ultrasound tumor volumes and margins," *J. Clin. Ultrasound* **22**(1), 29–36 (1994).
17. N. Dorward, O. Alberti, B. Velani, F. Gerritsen, W. Harkness, N. Kitchen, and D. Thomas, "Postimaging brain distortion: magnitude, correlates, and impact on neuronavigation," *J. Neurosurg.* **88**(4), 656–662 (1998).
18. D. Hill, C. J. Maurer, R. Maciunas, J. Barwise, J. Fitzpatrick, and M. Wang, "Measurement of intraoperative brain surface deformation under a craniotomy," *Neurosurgery* **43**(3), 514–526 (1998).
19. G. E. Keles, K. R. Lamborn, and M. S. Berger, "Coregistration accuracy and detection of brain shift using intraoperative sononavigation during resection of hemispheric tumors," *Neurosurgery* **53**(3), 556–562; discussion 562–554 (2003).
20. L. M. Auer and V. v. Velthoven, *Intraoperative Ultrasound Imaging in Neurosurgery: Comparison with CT and MRI*, Springer-Verlag, Berlin (1990).
21. J. E. Knake, R. A. Bowerman, T. M. Silver, and S. McCracken, "Neurosurgical applications of intraoperative ultrasound," *Radiol. Clin. North Am.* **23**, 656–662 (1985).
22. J. Sosna, M. M. Barth, J. B. Kruskal, and R. A. Kane, "Intraoperative sonography for neurosurgery," *J. Ultrasound. Med.* **24**(12), 1671–1682 (2005).
23. S. A. Toms, W.-C. Lin, R. J. Weil, M. D. Johnson, E. D. Jansen, and A. Mahadevan-Jansen, "Intraoperative optical spectroscopy identifies infiltrating glioma margins with high sensitivity," *Neurosurgery* **57**(4 Suppl.), 382–391 (2005).
24. W.-C. Lin, S. A. Toms, M. Johnson, E. D. Jansen, and A. Mahadevan-Jansen, "In vivo brain tumor demarcation using optical spectroscopy," *Photochem. Photobiol.* **73**(4), 396–402 (2001).
25. R. Andrews, R. Mah, A. Aghevli, K. Freitas, A. Galvagni, M. Guerrero, R. Papsin, C. Reed, and D. Stassinopoulos, "Multimodality stereotactic brain tissue identification: the NASA smart probe project," *Stereotact. Funct. Neurosurg.* **73**(1–4), 1–8 (1999).
26. A. C. Croce, S. Fiorani, D. Locatelli, R. Nano, M. Ceroni, F. Tancioni, E. Giombelli, E. Benericetti, and G. Bottiroli, "Diagnostic potential of autofluorescence for an assisted intraoperative delineation of glioblastoma resection margins," *Photochem. Photobiol.* **77**(3), 309–318 (2003).
27. L. Marcu, J. A. Jo, P. V. Butte, W. H. Yong, B. K. Pikul, K. L. Black, and R. C. Thompson, "Fluorescence lifetime spectroscopy of glioblastoma multiforme," *Photochem. Photobiol.* **80**, 98–103 (2004).
28. T. Vo-Dinh, D. L. Stokes, M. B. Wabuyele, M. E. Martin, J. M. Song, R. Jagannathan, E. Michaud, R. J. Lee, and X. Pan, "A hyperspectral imaging system for in vivo optical diagnostics. Hyperspectral imaging basic principles, instrumental systems, and applications of biomedical interest," *IEEE. Eng. Med. Biol. Mag.* **23**(5), 40–49(2004).
29. M. M. Haglund, M. S. Berger, and D. W. Hochman, "Enhanced optical imaging of human gliomas and tumor margins," *Neurosurgery* **38**(2), 308–317 (1996).
30. W. C. Lin, D. I. Sandberg, S. Bhatia, M. Johnson, G. Morrison, and J. Ragheb, "Optical spectroscopy for in-vitro differentiation of pediatric neoplastic and epileptogenic brain lesions," *J. Biomed.Opt.* **14**(1), 014028 (2009).
31. S. C. Gebhart, W. C. Lin, and A. Mahadevan-Jansen, "In vitro determination of normal and neoplastic human brain tissue optical properties using inverse adding-doubling," *Phys. Med. Biol.* **51**(8), 2011–2027 (2006).
32. H. Stepp, T. Beck, T. Pongratz, T. Meinel, F.W. Kreth, J. Tonn, and W. Stummer, "ALA and malignant glioma: fluorescence-guided resection and photodynamic treatment," *J. Environ. Pathol. Toxicol. Oncol.* **26**(2), 157–164 (2007).
33. H. R. Eggert and V. Blazek, "Optical properties of human brain tissue, meninges, and brain tumors in the spectral range of 200 to 900 nm," *Neurosurgery* **21**(4), 459–464 (1987).
34. Y. Ti and W. C. Lin, "Effects of probe contact pressure on in vivo optical spectroscopy," *Opt. Express* **16**(6), 4250–4262 (2008).
35. R. Reif, M. S. Amorosino, K. W. Calabro, O. A'Amar, S. K. Singh, and I. J. Bigio, "Analysis of changes in reflectance measurements on biological tissues subjected to different probe pressures," *J. Biomed. Opt.* **13**(1), 010502 (2008).